Complex variable element solution of potential flow problems using Taylor series for error analysis

T. V. Hromadka II

Department of Mathematics, California State University, Fullerton, CA, USA

R. J. Whitley

Department of Mathematics, University of California, Irvine, CA, USA

The complex variable boundary element method (CVBEM) is a numerical approach to solving boundary value problems of two-dimensional Laplace and Poisson equations. The CVBEM estimator exactly solves the governing partial differential equations in the problem domain but only approximately satisfies the problem boundary conditions. In this paper a new CVBEM error measure is used in aiding in the development of improved CVBEM approximators. The new approach utilizes Taylor series theory and can be readily programmed into computer software form. On the basis of numerous test applications it appears that use of this new CVBEM error measure leads to the development of significantly improved CVBEM approximation functions.

Keywords: complex variable boundary element method, Taylor series, error analysis, potential flow problems

1. Introduction

The objective in using the complex variable boundary element method (CVBEM) is to approximate analytic complex functions. Given that ω is a complex function which is analytic over a simply connected domain Ω with boundary values $\omega(\zeta)$ for $\zeta \in \Gamma$ (Γ is a simple closed contour), then both the real (ϕ) and the imaginary (ψ) parts of $\omega = \phi + i\psi$ satisfy the Laplace equation over Ω. Thus two-dimensional potential flow problems can be approximated by the CVBEM, including steady-state heat transport, soil water flow, plane stress, and elasticity.

The development of the CVBEM for engineering applications is detailed by Hromadka and Lai.[1] The CVBEM is a boundary integral technique, and consequently, a literature review of this class of numerical methods can be found in works such as the one by Lapidus and Pinder.[2] The Laplace and Poisson equations have been solved numerically with a high rate of convergence by the finite element, finite difference, and real variable boundary element methods.[2] However, issues regarding conditioning of the stiffness matrix for cases of small discretization remain open. The CVBEM results in a well-conditioned matrix system that may provide an alternative to highly discretized conditioning problems.

In this paper the CVBEM is expanded as a generalized Fourier series but introduces the use of Taylor series defined on each boundary element, expanded with respect to each nodal point. Boundary conditions are approximated in a "mean-square" error sense in that a vector space norm is defined which is analogous to the l_2 norm and then minimized by the selection of complex coefficients to be associated to each nodal point located on the problem boundary, Γ. For problems in which the boundary condition values are values of a function analytic on $\Omega \cup \Gamma$ the CVBEM approximation function converges almost everywhere (ae) on Γ.

The CVBEM generalized Fourier series approach will be developed before the development of the numerical technique is presented. To keep the paper concise, the development of the CVBEM approach, the definition of the working vector spaces, proofs of convergence of the generalized Fourier series expansion, and the proof of boundary condition convergence are all briefly presented.

Address reprint requests to Prof. Hromadka at the Dept. of Mathematics, California State University, Fullerton, CA 92634, USA.

Received 16 April 1991; revised 15 October 1991; accepted 12 November 1991

In this paper a new CVBEM error measure is used in aiding in the development of improved CVBEM approximators. The new approach utilizes Taylor series theory and can be readily programmed into computer software form. This new approximation error evaluation technique provides a convenient-to-use measure in improving CVBEM models by further discretization.

1.1. Definition of working space, $\mathbf{W}_\Omega$

Let Ω be a simply connected convex domain with a simple closed piecewise linear boundary Γ with centroid located at $0 + 0i$. Then in this paper, $\omega \in \mathbf{W}_\Omega$ has the property that $\omega(z)$ is analytic over $\Omega \cup \Gamma$.

1.2. Definition of the function $\|\omega\|$

For $\omega \in \mathbf{W}_\Omega$ the symbol $\|\omega\|$ is notation for

$$\|\omega\| = \left[\int_{\Gamma_\phi} (\mathrm{Re}\,\omega)^2\, d\mu + \int_{\Gamma_\psi} (\mathrm{Im}\,\omega)^2\, d\mu\right]^{1/2}$$

where both Γ_ϕ and Γ_ψ are a finite number of subsets of Γ that intersect only at a finite number of points in Γ.

The symbol $\|\omega\|_p$ for $\omega \in \mathbf{W}_\Omega$ is notation for

$$\|\omega\|_p = \left[\int_\Gamma |\omega(\zeta)|^p\, d\mu\right]^{1/p} \qquad p \geq 1$$

Of importance is the case of $p = 2$:

$$\|\omega\|_2 = \left[\int_\Gamma ([\mathrm{Re}\,\omega]^2 + [\mathrm{Im}\,\omega]^2)\, d\mu\right]^{1/2}$$

1.3. Almost-everywhere (ae) equality

A property that applies everywhere on a set E except for a subset E' in E such that the Lebesgue measure $\mathbf{m}(E') = 0$ is said to apply almost everywhere (ae). Because sets of measure zero have no effect on integration, almost-everywhere equality on Γ indicates the same class of element. Thus for $\omega \in \mathbf{W}_\Omega$, $[\omega] = \{\omega \in \mathbf{W}_\Omega : \omega(\zeta)$ are equal ae for $\zeta \in \Gamma\}$. For example, $[0] = \{\omega \in \mathbf{W}_\Omega : \omega(\zeta) = 0$ ae, $\zeta \in \Gamma\}$. When understood, the notation [ ] will be dropped.

2. Mathematical development

The H^p spaces (or Hardy spaces) are well documented in the literature.[3] Of special interest are the $E^p(\Omega)$ spaces of complex valued functions. If $\omega \in \mathbf{E}^2(\Omega)$, then ω satisfies the conditions of the definition of working space on $\mathbf{W}_\Omega$, where $\|\omega(\delta\zeta)\|_2$ is bounded as $\delta \to 1$. Finally, if $\omega \in \mathbf{E}^2(\Omega)$, then the Cauchy integral representation of $\omega(z)$ for $z \in \Omega$ applies. It is seen that $\mathbf{W}_\Omega \subset \mathbf{E}^2(\Omega)$.

2.1. Theorem (boundary integral representation)

Let $\omega \in \mathbf{W}_\Omega$ and $z \in \Omega$. Then

$$\omega(z) = \frac{1}{2\pi i}\int_\Gamma \frac{\omega(\zeta)\, d\zeta}{\zeta - z}$$

Proof

For $\omega \in \mathbf{W}_\Omega$, then $\omega \in \mathbf{E}^2(\Omega)$, and the result follows immediately.

2.2. Almost-everywhere (ae) equivalence

For $\omega \in \mathbf{W}_\Omega$, functions $x \in \mathbf{W}_\Omega$ equal to ω ae on Γ represent an equivalence class of functions which may be noted as $[\omega]$. Therefore functions x and y in $\mathbf{W}_\Omega$ are in the same equivalence class when

$$\int_\Gamma |x - y|\, d\mu = 0$$

For simplicity, $\omega \in \mathbf{W}_\Omega$ is understood to indicate $[\omega]$. This follows directly from the fact that integrals over sets of measure zero have no effect on the integral value.

2.3. Theorem (uniqueness of zero element in $\mathbf{W}_\Omega$*)*

Let $\omega \in \mathbf{W}_\Omega$ and $\phi = 0$ ae on Γ_ϕ and $\psi = 0$ ae on Γ_ψ. Then $(\omega,\omega) = 0 \Rightarrow \omega = [0]$.

Green's theorem states, let F and G be continuous and have continuous first and second partial derivatives in a simply connected region R bounded by a simple closed curve C. Then

$$\oint_C F\left(\frac{\partial G}{\partial y}dx - \frac{\partial G}{\partial x}dy\right) = -\int_R\int\left[F\left(\frac{\partial^2 G}{\partial x^2} + \frac{\partial^2 G}{\partial y^2}\right) + \left(\frac{\partial F}{\partial x}\frac{\partial G}{\partial x} + \frac{\partial F}{\partial y}\frac{\partial G}{\partial y}\right)\right] dx\, dy$$

Let $F = \phi$, $G = \phi$. Then

$$\int_\Gamma \phi\frac{\partial\phi}{\partial n}d\Gamma = \int_\Omega \phi\nabla^2\phi\, d\Omega + \int_\Omega\left[\left(\frac{\partial\phi}{\partial x}\right)^2 + \left(\frac{\partial\phi}{\partial y}\right)^2\right] d\Omega$$

But $\nabla^2\phi = 0$ in Ω. Thus

$$\int_\Gamma \phi\frac{\partial\phi}{\partial n}d\Gamma = \int_\Omega [\phi_x^2 + \phi_y^2]\, d\Omega$$

But $(\omega,\omega) = 0$ implies $\phi = 0$ on Γ_ϕ and $\psi = 0$ on Γ_ψ (hence $\partial\psi/\partial s = 0 \Rightarrow \partial\phi/\partial n = 0$), and

$$\underbrace{\int_{\Gamma_\phi} \phi\,\phi_n\, d\Gamma}_{0} + \underbrace{\int_{\Gamma_\psi} \phi\,\phi_n\, d\Gamma}_{0} = \int_\Omega (\phi_x^2 + \phi_y^2)\, d\Omega$$

Thus $(\omega,\omega) = 0 \Rightarrow \phi_x = 0 = \phi_y$ on Ω.

Thus $\phi(x,y)$ is a constant in Ω. But

$$\lim_{z\to\zeta\in\Gamma_\phi} \phi = 0 \Rightarrow \phi = 0$$

Similarly, $\psi = 0$. Thus $\omega = [0]$.

2.4. Theorem ($\mathbf{W}_\Omega$ *is vector space*)

$\mathbf{W}_\Omega$ is a linear vector space over the field of real numbers.

Proof

This follows directly from the character of analytic functions. The sum of analytic functions is analytic, and scalar multiplication of analytic functions is analytic. The zero element has already been noted by [0] in theorem 2.3.

2.5. Theorem (*definition of the inner product*)

Let $x, y, z, \in \mathbf{W}_\Omega$. Define a real-valued function (x,y) by

$$(x,y) = \int_{\Gamma_\Omega} \mathrm{Re}\, x \,\mathrm{Re}\, y \, d\mu + \int_{\Gamma_\psi} \mathrm{Im}\, x \,\mathrm{Im}\, y \, d\mu$$

Then $(\ ,\ )$ is an inner product over $\mathbf{W}_\Omega$.

Proof

It is obvious that $(x,y) = (y,x)$; $(kx,y) = k(x,y)$ for k real; $(x + y,z) = (x,z) + (y,z)$; and $(x,x) = \|x\| \geq 0$. By theorem 2.3, $(x,x) = 0$ implies Re $x = 0$ ae on Γ_ϕ and Im $x = 0$ ae on Γ_ψ and $x = [0] \in \mathbf{W}_\Omega$.

Three theorems follow immediately from the above, and hence no proof is given.

2.6. Theorem ($\mathbf{W}_\Omega$ *is an inner product space*)

For the defined inner product, $\mathbf{W}_\Omega$ is an inner product space over the field of real numbers.

3. The CVBEM and $\mathbf{W}_\Omega$

3.1. Definition of Λ

Let the number of angle points of Γ be noted as Λ. By a nodal partition of Γ, nodes $\{P_j\}$ with coordinates $\{z_j\}$ are defined on Γ such that a node is located at each vertex of Γ and the remaining nodes are distributed on Γ. Nodes are numbered sequentially in a counterclockwise direction along Γ. The scale of the partition is indicated by l, where $l = \max |z_{j+1} - z_j|$. Note that no two nodal points have the same coordinates in Γ.

3.2. Definition of Γ_j

A boundary element Γ_j is the line segment joining nodes z_j and z_{j+1}; $\Gamma_j = \{z: z = z(t) = z_j(1 - t) + z_{j+1}t, 0 \leq t \leq 1\}$. (Note for m nodes on Γ that $z_{m+1} = z_1$.)

3.3. Discretization of Γ *into CVBEs*

Let a nodal partition be defined on Γ. Then

$$\Gamma = \bigcup_{i=1}^{m} \Gamma_j$$

where m is the number of complex variable boundary elements (CVBEs).

3.4. Definition of $\mathbf{N}_j(\zeta)$

A linear basis function $\mathbf{N}_j(\zeta)$ is defined for $\zeta \in \Gamma$ by

$$\mathbf{N}_j(\zeta) = \begin{cases} (\zeta - z_{j-1})/(z_j - z_{j-1}) & \zeta \in \Gamma_{j-1} \\ (z_{j+1} - \zeta)/(z_{j+1} - z_j) & \zeta \in \Gamma_j \\ 0 & \zeta \notin \Gamma_{j-1} \cup \Gamma_j \end{cases}$$

The value of $\mathbf{N}_j(\zeta)$ is found to be real and bounded as indicated by the next theorem.

3.5. Theorem

Let $\mathbf{N}_j(\zeta)$ be defined for node $P_j \in \Gamma$. Then $0 \leq \mathbf{N}_j(\zeta) \leq 1$.

3.6. Definition of $G_m(\zeta)$

Let a nodal partition of m nodes $\{P_j\}$ be defined on Γ with $m \geq \Lambda$ and with scale l. At each node P_j, define nodal values $\bar{\omega}_j = \bar{\phi}_j + i\bar{\psi}_j$, where $\bar{\phi}_j$ and $\bar{\psi}_j$ are real numbers. A global trial function $G_m(\zeta)$ is defined on Γ for $\zeta \in \Gamma$ by

$$G_m(\zeta) = \sum_{j=1}^{m} \mathbf{N}_j(\zeta)\bar{\omega}_j$$

3.7. Theorem

From definition 3.6, $G_m(\zeta)$ is the sum of integrable continuous functions, and hence (a) $G_m(\zeta)$ is continuous on Γ and (b) for $\omega(\zeta) \in \mathbf{W}_\Omega$, $\omega(\zeta) \in L^2(\Gamma)$.

3.8. Discussion

As a result of $\omega(\zeta) \in L^2(\Gamma)$, then $\omega(\zeta)$ is measurable on Γ, and for every $\epsilon > 0$ there exists a continuous complex-valued function $g(\zeta)$ such that

$$\|\omega(\zeta) - g(\zeta)\|_1 < \epsilon/2$$

Choosing $G_m(\zeta)$ to approximate $g(\zeta)$ by

$$\|G_m(z) - g(z)\|_1 < \epsilon/2$$

then

$$\|\omega(\zeta) - G_m(\zeta)\|_1 < \|\omega(\zeta) - g(\zeta)\|_1 + \|g(\zeta) - G(\zeta)\|_1 < \epsilon$$

The CVBEM approximation function, $\hat{\omega}_m(z)$, is developed from $G_m(z)$ for m nodes on Γ by

$$\hat{\omega}_m(z) = \frac{1}{2\pi i}\int_\Gamma \frac{G_m(\zeta)\,d\zeta}{\zeta - z} \qquad z \in \Omega \tag{1}$$

where the $\bar{\omega}_j$ values used in $G_m(\zeta)$ are given by $\bar{\omega}_j = \omega(z_j)$, $\omega \in \mathbf{W}_\Omega$.

3.9. Theorem

Let $\omega \in \mathbf{W}_\Omega$. For $\epsilon > 0$ there exists a $G(\zeta)$ such that $\|\omega(\zeta) - G(\zeta)\|_1 < \epsilon$.

Proof follows from the discussion in section 3.8.

3.10. Theorem

Let $\omega \in \mathbf{W}_\Omega$ and $z \in \Omega$. For every $\epsilon > 0$ there exists a CVBEM approximation $\hat{\omega}_m(z)$ such that $|\omega(z) - \hat{\omega}_m(z)| < \epsilon$.

Proof

Let $d = \min |\zeta - z|$, $\zeta \in \Gamma$. Then for a global trial function $G_m(\zeta)$ defined on Γ,

$$|\omega(z) - \hat{\omega}_m(z)| = \left| \frac{1}{2\pi i} \int_\Gamma \frac{[\omega(\zeta) - G_m(\zeta)]\, d\zeta}{\zeta - z} \right| \leq \frac{1}{2\pi i} \|\omega - G_m\|_1$$

Choosing G_m (see section 3.8) such that $\|\omega - G_m\|_1 < 2\pi\, d\epsilon$ guarantees the desired result.

4. Taylor series expansions on CVBEs

4.1. Construction

Let $\omega \in \mathbf{W}_\Omega$. Then ω is analytic on an open domain Ω^A such that $\Omega \cup \Gamma$ is entirely contained in the interior of Ω^A. Let Γ^* be in Ω^A such that Γ^* is a finite length simple closed contour that is exterior to $\Omega \cup \Gamma$. Then ω is analytic on Γ^*, and by the maximum modulus theorem,

$$|\omega(z)| \leq M \qquad z \in \Gamma^* \tag{2}$$

for some positive constant M.

Also,

$$|\omega(z)| \leq M \qquad z \in \Omega \cup \Gamma \tag{3}$$

Define a nodal partition of m nodes on Γ. Complex variable boundary elements are defined to be the straight line segments $\Gamma_j = [z_j, z_{j+1}]$ where, for m nodes, $z_{m+1} \equiv z_1$. At the midpoint $\bar{z}_j = \frac{1}{2}(z_j + z_{j+1})$ of each Γ_j, expand $\omega(z)$ into a Taylor series $T_j(z - z_j)$. Each $T_j(z - \bar{z}_j)$ has a nonzero radius of convergence R_j, and $T_j(z - \bar{z}_j) = \omega(z)$ in the interior of circle $C_j = \{z : |z - \bar{z}_j| = R_j\}$. The C_j all minimally have radii R, where $R = \min |\zeta_1 - \zeta_2|$ such that $\zeta_1 \in \Gamma$ and $\zeta_2 \in \Gamma^*$. Descretize Γ into m CVBEs, Γ_j, $j = 1, 2, \ldots, m$, such that the length of Γ_j, $\|\Gamma_j\| \leq 2L/m$ where $L = \int_\Gamma |d\zeta|$ and $2L/m < R$, and the other conditions regarding placement of nodes at angle points of Γ are satisfied.

4.2. Taylor series expansion

For $\zeta \in \Gamma_j$,

$$T_j(\zeta - \bar{z}_j) = P_j^N(\zeta) + E_j^N(\zeta) \tag{4}$$

where N is the polynomial degree, and from Cauchy's theorem,

$$E_j^N(\zeta) = \frac{1}{2\pi i} \int_{C_j} \left(\frac{\zeta - \bar{z}_j}{z - \bar{z}_j} \right)^{N+1} \frac{\omega(z)\, dz}{z - \zeta} \tag{5}$$

The magnitude of $|E_j^N(\zeta)|$ is, for every j,

$$|E_j^N(\zeta)| \leq \frac{1}{2\pi} \left| \frac{\zeta - \bar{z}_j}{z - \bar{z}_j} \right|^{N+1} \frac{\max |\omega(z)| 2\pi R}{\min |z - \zeta|} \qquad z \in C_j \quad \zeta \in \Gamma \tag{6}$$

But

$$\left| \frac{\zeta - z_j}{z - \bar{z}_j} \right|^{N+1} \leq \left(\frac{L/m}{R} \right)^{N+1}$$

and thus

$$|E_j^N(\zeta)| \leq \frac{1}{2\pi} \left(\frac{L}{mR} \right)^{N+1} \frac{M 2\pi R}{R/2} = 2M \left(\frac{L}{mR} \right)^{N+1} \tag{7}$$

which is a result independent of j. Note that as the partition of Γ into CVBEs becomes finer, i.e., max $\|\Gamma_j\| \to 0$, then $m \to \infty$ and $|E_j^N(\zeta)| \to 0$. Also, as the order of the Taylor series polynomial increases, $N \to \infty$, and recalling that $(L/m) < R/2$, then $|E_j^N(\zeta)| \to 0$.

4.3. CVBEM error analysis

From Cauchy's theorem, for $z \in \Omega$,

$$\omega(z) = \frac{1}{2\pi i} \int_\Gamma \frac{\omega(\zeta)\, d\zeta}{\zeta - z} \tag{8}$$

On Γ, let

$$\omega(\zeta) = \sum_{j=1}^{m} \mathrm{X}_j T_j(\zeta) \qquad \zeta \in \Gamma \tag{9}$$

where X_j is the j-element characteristic function (i.e., $\mathrm{X}_j = 1$ for $\zeta \in \Gamma_j$; 0, otherwise). Then for $z \in \Omega$,

$$\omega(z) = \frac{1}{2\pi i} \int_\Gamma \frac{\sum_{j=1}^{m} \mathrm{X}_j T_j(\zeta)\, d\zeta}{\zeta - z} = \sum_{j=1}^{m} \frac{1}{2\pi i} \int_{\Gamma_j} \frac{T_j(\zeta)\, d\zeta}{\zeta - z} \tag{10}$$

For $T_j(\zeta) = P_j^N(\zeta) + E_j^N(\zeta)$,

$$\omega(z) = \frac{1}{2\pi i} \sum_{j=1}^{m} \int_{\Gamma_j} \frac{P_j^N(\zeta)\, d\zeta}{\zeta - z} + \frac{1}{2\pi i} \sum_{j=1}^{m} \int_{\Gamma_j} \frac{E_j^N(\zeta)\, d\zeta}{\zeta - z} = \hat{\omega}_N(z) + E_N(z) \tag{11}$$

The $\hat{\omega}_N(z)$ is the CVBEM approximation based on order N polynomials, where it is understood m nodes are used. The error, $E_N(z)$, is evaluated in magnitude for $z \in \Omega$ and using (12) to be

$$|E_N(z)| = \frac{1}{2\pi} \left| \sum_{j=1}^{m} \int_{\Gamma_j} \frac{E_j^N(\zeta)\, d\zeta}{\zeta - z} \right| \leq \frac{1}{2\pi} \frac{(m)(\max \|\Gamma_j\|)(\max |E_j^N(\zeta)|)}{\min |\zeta - z|} = \frac{\left(\frac{m}{2\pi}\right)\left(\frac{2L}{m}\right)\left(2M\left[\frac{L}{mR}\right]^{N+1}\right)}{D} = \frac{2LM}{\pi D}\left(\frac{L}{mR}\right)^{N+1} \tag{12}$$

where $D = \min |\zeta - z|$ for $\zeta \in \Gamma$.

Recalling that $(L/m) < R/2$, $|E_N(z)| \to 0$ as either $m \to \infty$ or $N \to \infty$. Thus as the number m of CVBEs increases, or the order of the interpolating polynomial N increases, error $|E_N(z)| \to 0$.

4.4. CVBEM numerical analog

As $z \to \zeta \in \Gamma_j$, for $z \in \Omega$, then $\omega(z) \to \omega(\zeta) = T_j(\zeta)$.

The CVBEM procedure is to set in a Cauchy limit sense,

$$T_j(z) = \frac{1}{2\pi i} \sum_{j=1}^{m} \int_{\Gamma_j} \frac{T_j(\zeta)\, d\zeta}{\zeta - z} \tag{13}$$

as $z \to \Gamma$ while $z \in \Omega$.

For order N Taylor series expansions the CVBEM sets in the Cauchy limit

$$P_j^N(z) = \frac{1}{2\pi i} \sum_{j=1}^{m} \int_{\Gamma_j} \frac{P_j^N(\zeta)\, d\zeta}{\zeta - z} \tag{14}$$

as $z \to \Gamma$ while $z \in \Omega$.

If collocation is used, the numerical approach is to set[1]

$$P_j^N(z_i) = \omega(z_i) \tag{15}$$

for each nodal coordinate $z_i \in \Gamma_j$.

If a least-squares approach is used, the numerical approach is to minimize[4]

$$\|P_j^N(\zeta) - \omega(\zeta)\| \qquad \zeta \in \Gamma \qquad j = 1, 2, \ldots, m \tag{16}$$

Letting

$$G_m(\zeta) = \sum_{j=1}^{m} N_j(\zeta)\, \bar{\omega}_j$$

where it is recalled $\bar{\omega}_j = \omega(z_j)$,

$$\lim_{l \to 0} G(\zeta) = \omega(\zeta)$$

and

$$\omega(\zeta) = \lim_{l \to 0} \frac{1}{2\pi i} \int_{\Gamma} \frac{G(\zeta)\, d\zeta}{\zeta - z} \qquad z \in \Omega \tag{17}$$

where l is the scale of the nodal partition of Γ.

5. Implementation

In general, one does not have both ϕ and ψ values defined on Γ but instead has ϕ values defined only on a portion of Γ, specified as Γ_ϕ, and ψ values defined only on the remaining portion of Γ, Γ_ψ, where $\Gamma_\phi \cup \Gamma_\psi = \Gamma$. That is, we have a mixed boundary value problem.

The numerical formulation given in the above equations solves for the unknown ψ values on Γ_ϕ and the unknown ϕ values on Γ_ψ. Once the unknown ϕ and ψ values are estimated, denoted as $\hat{\phi}$ and $\hat{\psi}$, then the global trial functions are well defined and can be used in $\hat{\omega}(z)$ estimates for the interior of Ω. The possible variations in such boundary condition issues are addressed by Hromadka and Lai.[1]

In this paper we focus upon the Taylor series expansions in each Γ_j, as the interpolation polynomial order, N, increases and also as the number of CVBEs, m, increases.

Thus the numerical approach used in the CVBEM computer program formulation is outlined by the following steps:

1. Discretize the problem boundary Γ (which is a finite union of straight line segments) into m CVBEs by use of nodal points distributed on Γ where minimally a node is placed at each corner of Γ; i.e., $m \geq \Lambda$.
2. For $N = 1$ a linear interpolating polynomial is defined on each Γ_j. For $N > 1$ a higher-order polynomial expansion is used, and consequently, additional interpolation nodes are defined in each Γ_j. For example, for $N = 2$ a midpoint node is added to each Γ_j; for $N = 3$, two additional nodes are defined in the interior of each Γ_j.
3. Given N, a matrix solution provides the coefficients needed to define interpolating polynomials for each CVBE, using splines.
4. The unknown nodal values are estimated by means of collocation or least-squares error minimization.
5. Using the estimates for the unknown nodal values, a CVBEM approximation $\hat{\omega}(z)$ is well defined for estimating $\omega(z)$ values in the interior of Ω.
6. CVBEM error is evaluated by comparing $\hat{\omega}(z)$ and $\omega(z)$ with respect to the known boundary values of $\omega(z)$ on Γ; that is, compare $\hat{\phi}$ to ϕ on Γ_ϕ, and compare $\hat{\psi}$ to ψ on Γ_ψ. (From the previous mathematical development, if $\hat{\phi} = \phi$ on Γ_ϕ and $\hat{\psi} = \psi$ on Γ_ψ, then $\hat{\omega}(z) = \omega(z)$ for all $z \in \Omega$, if $\omega \in \mathbf{W}_\Omega$.)
7. After $\hat{\omega}$ and ω are compared as to boundary condition values, then the CVBEM program user can decrease the partition scale (i.e., increase the number of nodes uniformly) and/or increase the CVBE interpolating polynomial order, N. The modelling goal is to increase (m,N) until the boundary conditions are well approximated by the CVBEM $\hat{\omega}(z)$. It is recalled that regardless of goodness of fit of $\hat{\omega}(z)$ to the problem boundary conditions, the components of $\hat{\omega}(z)$, i.e., the functions $\hat{\phi}(z)$ and $\hat{\psi}(z)$ (where $\hat{\omega}(z) = \hat{\phi}(z) + i\hat{\psi}(z)$) exactly satisfy the Laplacian $\nabla^2\hat{\phi} = 0$ and $\nabla^2\hat{\psi} = 0$ for all $z \in \Omega$. Thus there is no error in satisfying the Laplacian equation in Ω. This feature afforded by the CVBEM is not achieved by use of the usual finite element or finite difference numerical techniques, which have errors in satisfying the problem's boundary conditions as well as errors in satisfying the flow field Laplacian in Ω.
8. A new approach to evaluating CVBEM approximation error is to examine the closeness between values of the interpolating polynomial in each CVBE, and the CVBEM $\hat{\omega}(z)$ function, for z in Γ_j. That is, examine in a Cauchy limit $\|P_j^N(\zeta) - \hat{\omega}(\zeta)\|_2$, $\zeta \in \Gamma_j$, for all CVBE Γ_j. As $\|P_j^N(\zeta) - \hat{\omega}(\zeta)\|_2 \to 0$ (i.e., by increasing m and N) for all j and all $\zeta \in \Gamma_j$, then necessarily, $\hat{\omega}(z) \to \omega(z)$ for all $z \in \Omega$, if $\omega(z) \in \mathbf{W}_\Omega$.
9. The choice to increase m or N is made by increasing

both m and N in those boundary elements that have the most approximation error of $\|P_j^N(\zeta) - \hat{\omega}(\zeta)\|$ for $\zeta \in \Gamma_j$. In this way, $\hat{\omega}(z)$ approximations improve in accuracy without excessive additional computation. Generally, three or four attempts in developing $\hat{\omega}(z)$ functions may be needed for difficult potential flow problems, each successive CVBEM approximator being based upon the prior attempt but with localized increases in m and N where approximation error was largest.

6. Application

A CVBEM computer program was prepared that included the ability to increase the number of boundary elements by discretizing specific elements into more elements, and also to increase the interpolating function polynomial order, N, within specific boundary elements. The program included in its output the computation of $\|P_j^N(\zeta) - \omega(\zeta)\|_2$, $\zeta \in \Gamma_j$, for each boundary element.

For each CVBEM attempt, N is increased by 1 and the boundary element halved in length (to produce two elements) that had the largest values of $\|P_j^N(\zeta) - \omega(\zeta)\|_2$. The modelling process continues until a reasonable $\hat{\omega}(z)$ fit to the problem boundary conditions is achieved.

Applications demonstrating the CVBEM to numerically solve boundary value problems involving the two-dimensional Laplace or Poisson equation can be found in several publications.[1-5] The focus of this paper is the presentation of another CVBEM error evaluation technique that appears to provide a more robust guide in developing subsequent improved CVBEM approximators than the other techniques in use, such as the approximate boundary technique,[1] and the usual eye-fit comparisons between ϕ versus $\hat{\phi}$ on Γ_ϕ and ψ versus $\hat{\psi}$ on Γ_ψ.

In numerous test problems it was found that use of the $\|P^N(\zeta) - \hat{\omega}(\zeta)\|_2$ error to pinpoint localized CVBEM approximation error provided, in general, a better approach to improving CVBEM functions than the approximate boundary approach. The following problems demonstrate application of the $\|P_j^N(\zeta) - \omega(\zeta)\|_2$ error measure technique to locate where additional nodal points need to be added to Γ in order to develop more refined CVBEM approximations. In each application a mixed boundary value problem is defined by prescription of either ϕ, ψ, or $\partial\phi/\partial n$ along portions of Γ. The CVBEM is applied to an initial nodal point distribution along Γ, and then the error measure is evaluated for each boundary element. The boundary element that manifests the largest value of error is then further discretized, or the Taylor polynomial order increased by 1 (up to a maximum order of 8 in the prepared computer software). The program user selects, up front, the order of the Taylor polynomial to be used; the program conducts the discretization.

For each problem shown the exact solution used to generate the test problem is given. Initially, nodes are only defined to be located at the vertices of Γ. Also, a quadratic polynomial is used for each element. Thereafter the software generates successively finer CVBEM estimates, by discretization, by use of the error measure between $P_j^N(\zeta)$ and $\omega(\zeta)$ on Γ. The maximal error $E = \|\hat{\omega}(z) - \omega(z)\|$ is then computed for demonstration purposes, as $\omega(z)$ is known. Plots of error for 25- and 40-node discretization are provided for each application.

To demonstrate the error analysis procedures discussed above, two mixed boundary value problems are considered in which analytic solutions are known. A FORTRAN computer program, based on the complex variable boundary element method, which allows an increase in Taylor series polynomial order or an increase in nodal density is used.

For both problems considered, an initial nodal point scheme of 12 nodes is defined on each of the problem boundaries. Boundary conditions of specified stream function or specified potential function values are used (even though flux type boundary conditions are straightforward to include). A CVBEM approximation function is developed based on the initial nodal point placement, and streamlines are automatically generated and plotted as solid lines within the problem domain (recall the CVBEM develops a function $\hat{\omega}(x,y)$ inside the problem domain, Ω). For comparison purposes, associated streamlines for the analytic solution $\omega(z)$ also are plotted, as dashed lines, within Ω.

Because application of the CVBEM necessarily involves problems in which the exact solution is unknown, one of the two boundary condition function values is left "unknown" along the problem boundary. By using the error between the approximated boundary values and the known boundary values, additional CVBEM model complexity can be introduced. The errors computed are the usual integrated root-mean-square error and magnitude error. Plots of these errors, as computed along the problem boundary, are included in the application figures.

Subsequent CVBEM approximations, ultimately leading to use of 25 and 40 nodes on Γ, are shown in the attached figures, along with a comparison of streamlines between approximation and solution results, and the error plots. A quartic trail function is used in the 40-point discretization.

Application A

Solve $\partial^2\phi/\partial x^2 + \partial^2\phi/\partial y^2 = 0$ in Ω, where Ω is the domain shown in *Figure 1*. Stream function values are specified along the horizontal lines of Γ, and potential function values are specified along the horizontal lines of Γ, forming a mixed boundary value problem. The analytic solution used is $\omega(z) = \ln[(z + 1)/(z - 1)]$. *Figures 1, 2,* and *3* show approximation results versus exact values for 12-, 25-, and 40-boundary nodes, respectively. The accompanying figures show magnitude and integrated root-mean-square error plots along Γ for the boundary values.

Application B

Figure 4 solves the Laplace equation for ideal fluid flow over a cylinder on the shown domain, Ω. The

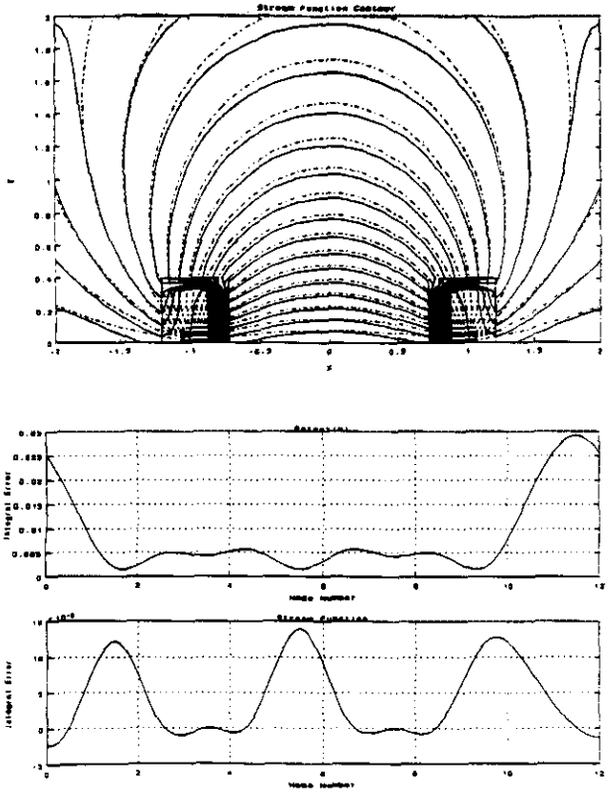

Figure 1. Application A with 12 nodes

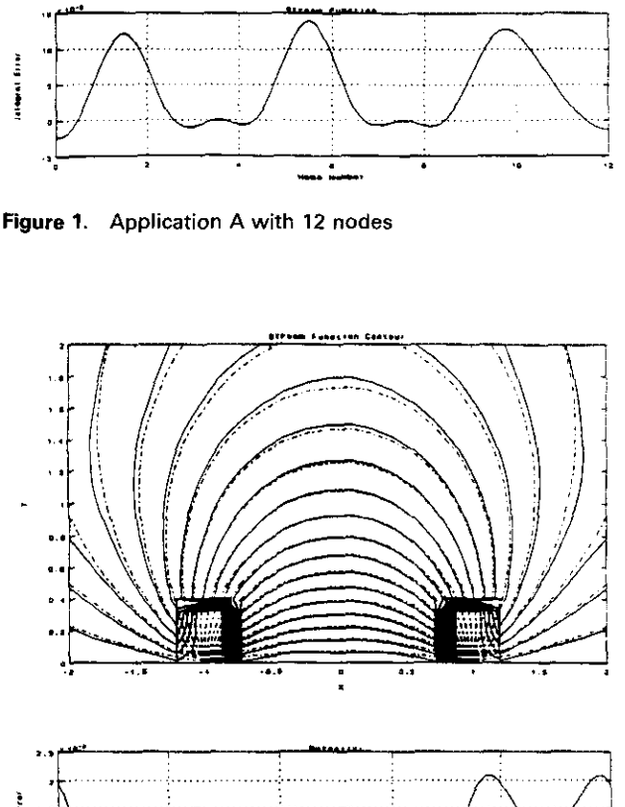

Figure 2. Application A with 25 nodes

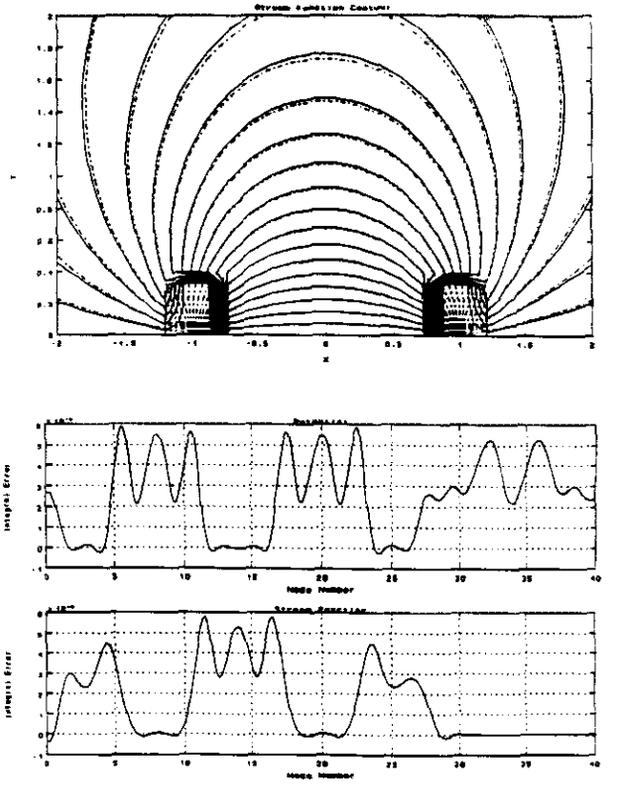

Figure 3. Application A with 40 nodes

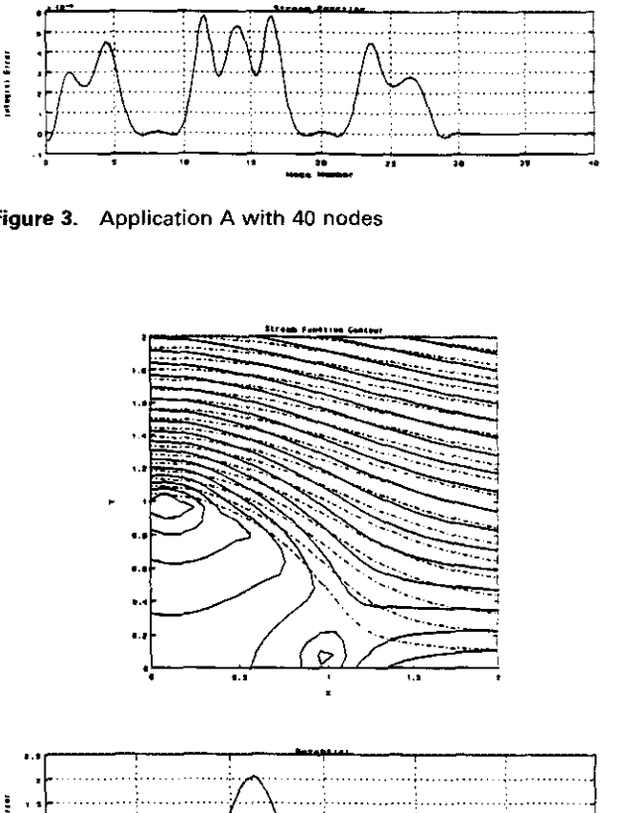

Figure 4. Application B with 12 nodes

CVBEM versus analytic results are compared in *Figures 4, 5,* and *6* for 12-, 25-, and 40-node placements, respectively. Also shown are corresponding error plots in meeting boundary condition values along Γ. The exact solution is $\omega(z) = z + 1/z$. Stream function values are specified along the arc and also on $x = 0$; otherwise, potential function values are specified along Γ.

Discussion of results

The two application problems demonstrate using two commonly employed error evaluation techniques in handling approximation error in meeting the problem boundary conditions. Because the CVBEM leads to exact solution of the partial differential equation, only boundary value approximation error exists. The approach to add CVBEM model complexification by either more nodes or higher Taylor series order expansions encompasses two viable techniques used in this paper. The complexification is added, however, where the boundary condition approximation error is relatively large.

Because the CVBEM develops a two-dimensional approximation function, precise flow nets can be developed inside the problem domain, which can be compared to known problem solutions when available. For example, *Figure 7* shows a plot of stream function values for Application A, while *Figures 8* and *9* show 25- and 40-node CVBEM approximations, respectively. *Figure 10* shows Application A, a state variable

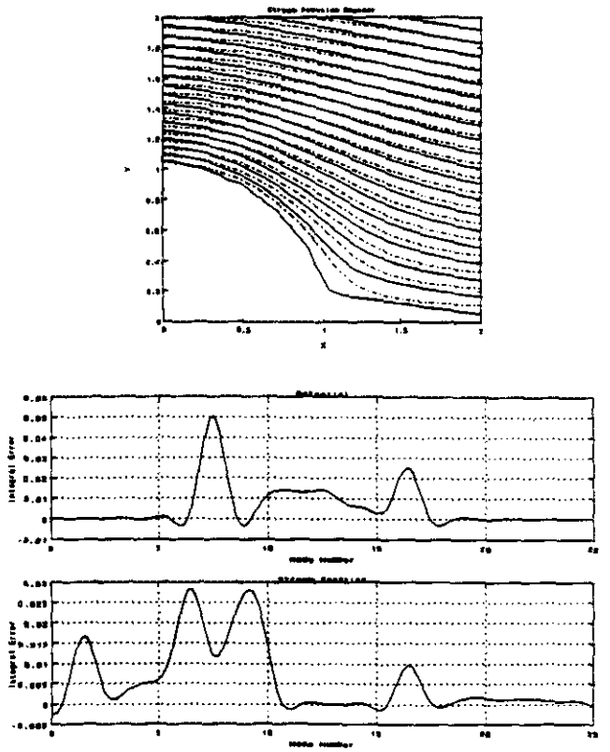

Figure 5. Application A with 25 nodes

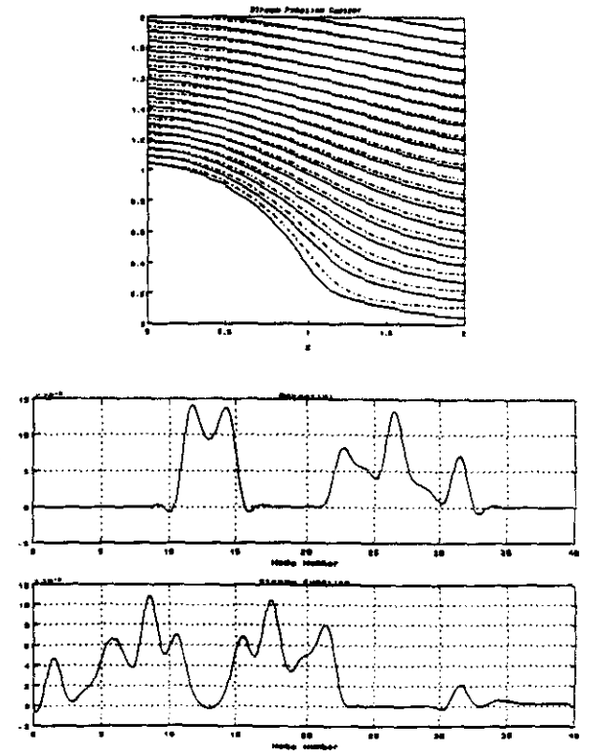

Figure 6. Application B with 40 nodes

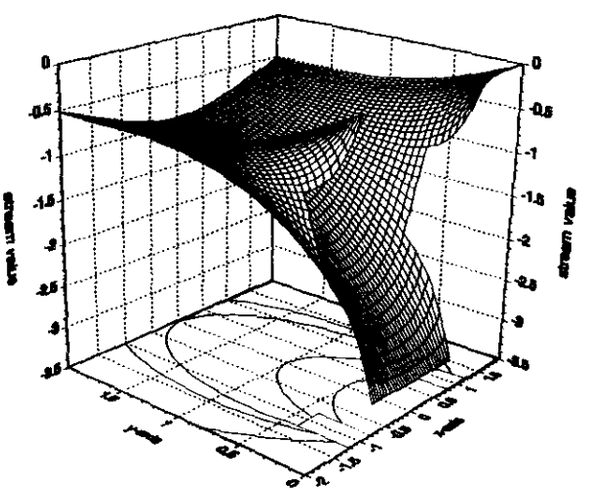

Figure 7. Stream function surface plot, ln [(z + 1)/(z − 1)]

plot, whereas *Figures 11* and *12* show 25- and 40-node CVBEM approximations.

The comparability of the approximated flow net to the solution's flow net is of importance due to the need for computing higher-order derivative functions from the CVBEM approximation function, $\hat{\omega}(z)$. For example, we know that $\hat{\omega}(z) = \hat{\phi}(x,y) + i\hat{\psi}(x,y)$ where $\nabla^2\hat{\phi} = 0$ and $\nabla^2\hat{\psi} = 0$ inside Ω. Then other differential quantities may be evaluated by directly differentiating $\hat{\omega}(z)$ (this differs from domain discretization techniques

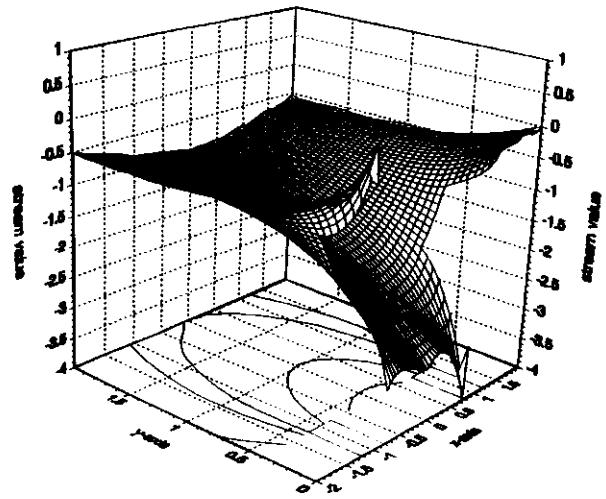

Figure 8. Stream function surface plot, 25-node approximation, ln $[(z + 1)/(z - 1)]$

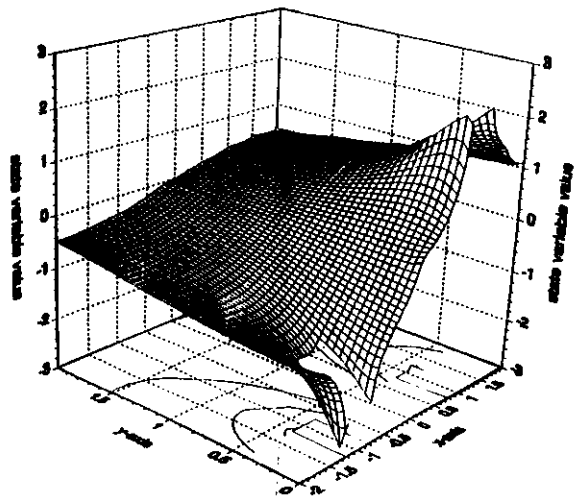

Figure 11. State variable surface plot, 25-node approximation, ln $[(z + 1)/(z - 1)]$

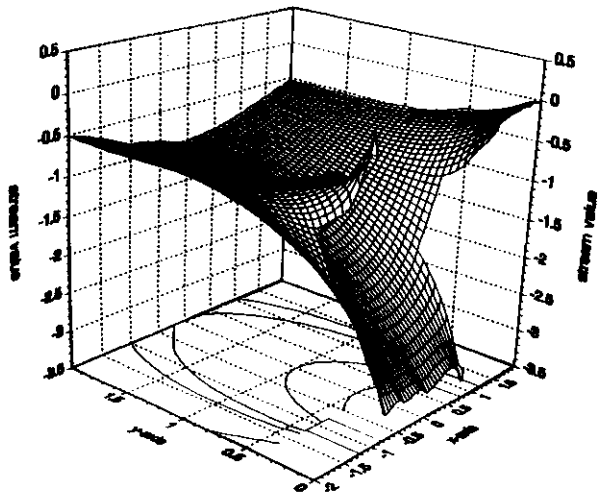

Figure 9. Stream function surface plot, 40-node approximation, ln $[(z + 1)/(z - 1)]$

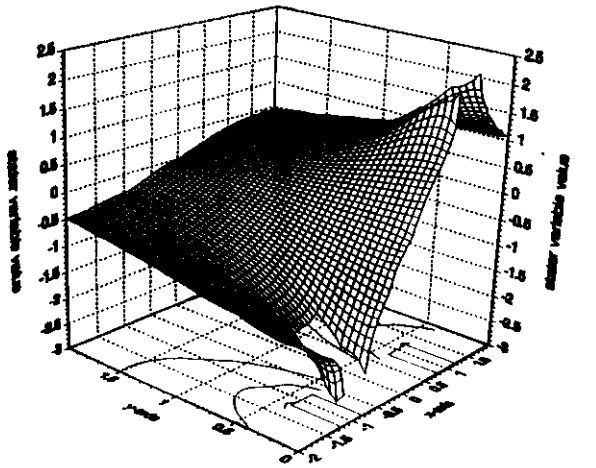

Figure 12. State variable surface plot, 40-node approximation, ln $[(z + 1)/(z - 1)]$

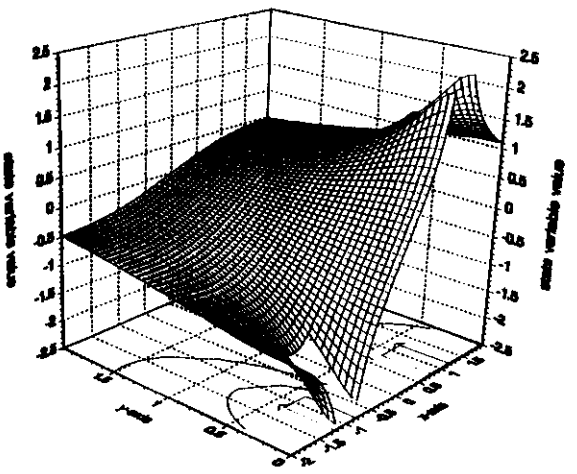

Figure 10. State variable surface plot, ln $[(z + 1)/(z - 1)]$

that use interpolation functions in the problem interior), resulting in a two-dimensional function defined inside Ω. For example, given $\hat{\omega}(z)$ for a mixed boundary value problem, $[d^m\hat{\omega}(z)]/dz^m$ is readily computed and evaluated for $z \in \Omega$.

7. Conclusions

The CVBEM is a numerical approach to solving boundary value problems of two-dimensional Laplace and Poisson equations. The CVBEM estimator exactly solves the governing partial differential equations in the problem domain but only approximately satisfies the problem boundary conditions. The CVBEM approximator can be improved by developing a better fit to the problem boundary conditions. In this paper a new CVBEM error measure is used in aiding in the development of improved CVBEM approximators. The new approach utilizes Taylor series theory and can be

readily programmed into computer software form. On the basis of numerous test applications it appears that use of this new CVBEM error measure leads to the development of significantly improved CVBEM approximation functions.

Notation

$d\mu$	$\lvert d\zeta\rvert$, $\zeta \in \Gamma$
L	length of Γ
l	max $\lvert z_{j+1} - z_j\rvert$
$N_j(\zeta)$	linear basis function defined on $\zeta \in \Gamma$
P_j	nodal point j, $P_j \in \Gamma$
z_c	centroid of $\Omega (z_c = 0 + 0i)$
$\{z_j\}$	nodal point coordinates defined on Γ
Γ	simple closed contour forming the boundary of Ω
Γ_j	boundary element (line segment) connecting nodal points with coordinates z_j, z_{j+1}
Γ_δ	$\{z \in \Omega: z = \delta\zeta, \zeta \in \Gamma\}$
Γ_ϕ, Γ_ψ	$\Gamma_\phi \cup \Gamma_\psi = \Gamma$ and $\Gamma_\phi \cap \Gamma_\psi$ at finite number of points. Here, ϕ is known on Γ_ϕ, and ψ is known on Γ_ψ, where $\omega = \phi + i\psi$. Both Γ_ϕ and Γ_ψ are simply connected contours
δ	a coordinate reduction factor, $0 < \delta < 1$
ζ, z	$\zeta \in \Gamma$, $z \in \Omega$; $\zeta = \mathrm{Re}^{i\theta}$ for $0 \le \theta < 2\pi$ (no two points ζ_1 and ζ_2 on Γ have the same angle θ)
θ_j	branch-cut angle of $\ln_j (z - z_j)$
Λ	number of angle points on Γ
ϕ	Re ω, $\omega = \phi + i\psi$
ψ	Im ω
Ω	convex, simply connected domain with centroid $0 + 0i$
$\overline{\Omega}$	$\Omega \cup \Gamma$
Ω_δ	$\{z \in \Omega: z$ enclosed by $\Gamma_\delta\}$
$\overline{\Omega}_\delta$	$\Omega_\delta \cup \Gamma_\delta$
$\lvert\omega\rvert$	$(\phi^2 + \psi^2)^{1/2}$
$\lVert\omega\rVert$	$(\int_{\Gamma_\phi}(\mathrm{Re}\ \omega)^2\, d\mu + \int_{\Gamma_\psi}(\mathrm{Im}\ \omega)^2\, d\mu)^{1/2}$
ω_j	nodal value $\omega(z_j)$, $\omega_j = \phi_j + i\psi_j$
$\overline{\omega}_j$	CVBEM approximation evaluated at $z_j \in \Gamma$
$\lVert\omega\rVert_p$	$(\int_\Gamma \lvert\omega(\zeta)\rvert^p\, d\mu)^{1/p}$
(ω,ω)	$\int_{\Gamma_\phi}(\mathrm{Re}\ \omega)^2\, d\mu + \int_{\Gamma_\psi}(\mathrm{Im}\ \omega)^2\, d\mu$

References

1 Hromadka, T. V., II and Lai, C. *The Complex Variable Boundary Element Method in Engineering Analysis*. Springer-Verlag, New York, 1987

2 Lapidus, L. and Pinder, G. F. *Numerical Solution of Partial Differential Equation in Science and Engineering*. John Wiley, New York, 1982

3 Duren, P. L. *Theory of H^p Spaces*. Academic, San Diego, CA, 1970

4 Hromadka, T. V., II and Whitley, R. J. Numerical approximation of linear operator equations using a generalized Fourier series: Ordinary and partial differential equations with boundary conditions. *Appl. Math. Modelling* 1989, **13**, 601–614

5 Mathews, J. H. *Basic Complex Variables for Mathematics and Engineering*. Allyn and Bacon, Boston, MA, 1982